OPEN

Electromagnetic Navigation Bronchoscopy With Tomosynthesis-based Visualization and Positional Correction

Three-dimensional Accuracy as Confirmed by Cone-Beam Computed Tomography

Michael A. Pritchett, DO, MPH, Krish Bhadra, MD,† and Jennifer S. Mattingley, MD‡*

Background: **Electromagnetic navigation bronchoscopy (ENB) aids in lung lesion biopsy. However, anatomic divergence between the preprocedural computed tomography (CT) and the actual bronchial anatomy during the procedure can limit localization accuracy. An advanced ENB system has been designed to mitigate CT-to-body divergence using a tomosynthesis-based software algorithm that enhances nodule visibility and allows for intraprocedural local registration.**

Materials and Methods: **A prospective, 2-center study was conducted in subjects with single peripheral lung lesions ≥ 10 mm to assess localization accuracy of the superDimension navigation system with fluoroscopic navigation technology. Three-dimensional accuracy was confirmed by cone-beam computed tomography. Complications were assessed through 7 days.**

Results: **Fifty subjects were enrolled (25 per site). Lesions were < 20 mm in 61.2% (30/49). A bronchus sign was present in 53.1% (26/49). Local registration was completed in 95.9% (47/49). Three-dimensional target overlap (primary endpoint) was achieved in 59.6% (28/47) and 83.0% (39/47) before and after location correction, respectively. Excluding subjects with unevaluable video files, target overlap was achieved 68.3% (28/41) and 95.1% (39/41), respectively. Malignant results were obtained in 53.1% (26/49) by rapid on-site evaluation and 61.2% (30/49) by final pathology of the ENB-aided sample. Diagnostic yield was not evaluated. Procedure-related complications were pneumothorax in 1 subject (no chest tube required) and scant hemoptysis in 3 subjects (no interventions required).**

Conclusion: **ENB with tomosynthesis-based fluoroscopic navigation improved the 3-dimensional convergence between the virtual target and actual lung lesion as confirmed by cone-beam computed tomography. Future studies are necessary to understand the impact of this technology on diagnostic yield.**

Key Words: electromagnetic navigation bronchoscopy, cone-beam computed tomography, tomosynthesis, fluoroscopic navigation, lung cancer

(*J Bronchol Intervent Pulmonol* 2021;28:10–20)

Electromagnetic navigation bronchoscopy (ENB) is a minimally invasive method to safely guide bronchoscopic tools to peripheral lung nodules. Diagnostic yields range from 67% to 84% in the majority of published ENB studies.[1] The prospective, multicenter NAVIGATE study reported a diagnostic yield of 73% in over 1000 patients.[2]

Most guided bronchoscopy systems, including electromagnetic platforms,[2,3] augmented fluoroscopy technologies,[4] virtual bronchoscopic navigation,[5–7] and robotic bronchoscopy[8,9] depend, at least in part, on preprocedural computed tomography (CT) scans to create a virtual lung map. When changes in lung anatomy occur between the preprocedural CT scan and the bronchoscopic procedure, the resulting "CT-to-body divergence" causes inaccurate

Received for publication December 16, 2019; accepted April 23, 2020.
From the *FirstHealth of the Carolinas and Pinehurst Medical Clinic, Pinehurst, NC; †CHI Memorial Rees Skillern Cancer Institute, Chattanooga, TN; and ‡Medtronic, Minneapolis, MN.
Presented as a late-breaking podium presentation at the CHEST annual meeting in New Orleans, LA on October 23, 2019 (Bhadra et al. *CHEST*. 2019;156:A2262–A2263).
Clinical Trial Registration Number: www.clinicaltrials.gov NCT03585959.
Western Institutional Review Board #20181181 (submitted April 9, 2018 and approved May 14, 2018).
Disclosure: Study sponsored and funded by Medtronic. M.A.P. discloses speaking, consulting, or research payments from Medtronic, Auris Health Inc., BodyVision, Intuitive Surgical, Philips, Biodesix, AstraZeneca, Johnson & Johnson/NeuWave, Boehringer-Ingleheim, United Therapeutics, Actelion, Inivata, and Boston Scientific. K.B. discloses consulting/speaking payments from Medtronic, Boston Scientific, BodyVision, Auris Health Inc., Intuitive Surgical, Veracyte, Biodesix, MeritMedical Endotek, and Johnson & Johnson. J.S.M. is a full-time employee of Medtronic.
Reprints: Michael A. Pritchett, DO, MPH, FirstHealth of the Carolinas and Pinehurst Medical Clinic, 205 Page Road, Pinehurst, NC 28374 (e-mail: mpritchett@pinehurstmedical.com).

DOI: 10.1097/LBR.0000000000000687

intraprocedural lesion localization and reduced diagnostic yield.[10–12]

Several advanced bronchoscopy platforms have been developed that attempt to mitigate CT-to-body divergence.[9,11,13–16] One new system uses intraprocedural tomosynthesis-based enhanced fluoroscopic navigation technology to improve lesion visibility and compensate for CT-to-body divergence with an integrated local registration feature that updates the relationship between the catheter and the lesion. The first published study of this system reported a higher procedure-day diagnostic yield, increasing from 54% to 79% ($P = 0.002$) compared with ENB without updated positioning using local registration.[17] However, diagnostic yield is often confounded by operator technique, choice of biopsy tools, lesion characteristics, and varied definitions. Navigation accuracy of new navigation technologies also requires a confirmation of 3-dimensional localization against ground truth, as measured by cone-beam computed tomography (CBCT). The current report is the first prospective, multicenter study of the tomosynthesis-based fluoroscopic navigation system, and evaluated the 3-dimensional localization accuracy as confirmed by CBCT.

MATERIALS AND METHODS

This study was conducted in accordance with the Declaration of Helsinki and all local regulatory requirements. The protocol was approved by the institutional review board of all participating sites. All subjects provided written informed consent.

Test Device

The superDimension navigation system version 7.2 with fluoroscopic navigation technology (Medtronic, Minneapolis, MN) is a minimally invasive approach to guide endoscopic tools to difficult to reach lung nodules or masses (Fig. 1).[18,19] The fluoroscopic navigation module incorporates a proprietary advanced algorithm that uses tomosynthesis[20,21] to reconstruct a 3-dimensional model from multiple 2-dimensional C-arm fluoroscopic images taken at various angles around the patient (Fig. 1D). Operators are also able to scroll through multiple fluoroscopic slices from different angles, minimizing the impact of any visual obstructions. This method provides enhanced visualization of nodules that might not have been visible on standard fluoroscopy (Figs. 1B, E). A local registration feature updates the relationship between the catheter tip and the target intraprocedurally, thus helping to correct CT-to-body divergence (Figs. 1F–H).

Study Procedures

A prospective, single-arm, 2-center, feasibility study was conducted to confirm the technical localization accuracy of ENB with fluoroscopic navigation. Eligible patients were those with a peripheral lung lesion, 10 mm or greater in diameter, amenable to ENB with biopsy. Central lesions visible endobronchially or reachable by flexible bronchoscopy or endobronchial ultrasound (EBUS) without ENB were excluded. All lesions were characterized as peripheral nodules in that they were surrounded by normal aerated lung, none were visible endobronchially, and all were beyond the segmental bronchus.[13] Lesions within 10 mm of the diaphragm were excluded. One lesion was assessed per subject.

An overview of the ENB with fluoroscopic navigation procedural method used at another institution has been published.[17] In standard practice, the procedure is conducted using C-arm fluoroscopy without the need for CBCT. For the purposes of this study, CBCT was used as ground truth to document the target lesion location and assess the localization accuracy of the fluoroscopic navigation system. Figure 2 shows the study-specific procedural steps. The operator first navigated to the target lesion, in a position that would be considered adequate to begin tissue sampling if local registration were not available. Fluoroscopy and CBCT sweeps were then conducted to analyze the 3-dimensional spatial relationship between the virtual target and the actual lesion before and after local registration.

Although not dictated by the clinical study protocol, both sites used ventilation strategies optimized to reduce motion and minimize atelectasis.[12] The ventilation protocols were not precisely identical between the 2 study sites but they were identical between sweeps (as detailed in Fig. 2). Incentive spirometry was used preprocedure to recruit lung volume and address existing atelectasis. The lowest tolerable FiO_2 was used for preoxygenation. General anesthesia, paralysis, and intubation were used reduce motion. Expeditious intubation (rather than traditional rapid sequence) was used to minimize atelectasis, with recruitment maneuvers performed immediately after intubation. Positive end-expiratory pressure was used from the preinduction phase and throughout the procedure[22,23] as tolerated hemodynamically and on the basis of lesion location, typically 8 to 15 cm H_2O or higher on the basis of patient and lesion characteristics (eg, morbid obesity).[23,24] Higher tidal volumes were used as tolerated to maintain optimal lung inflation. Breath-holds were

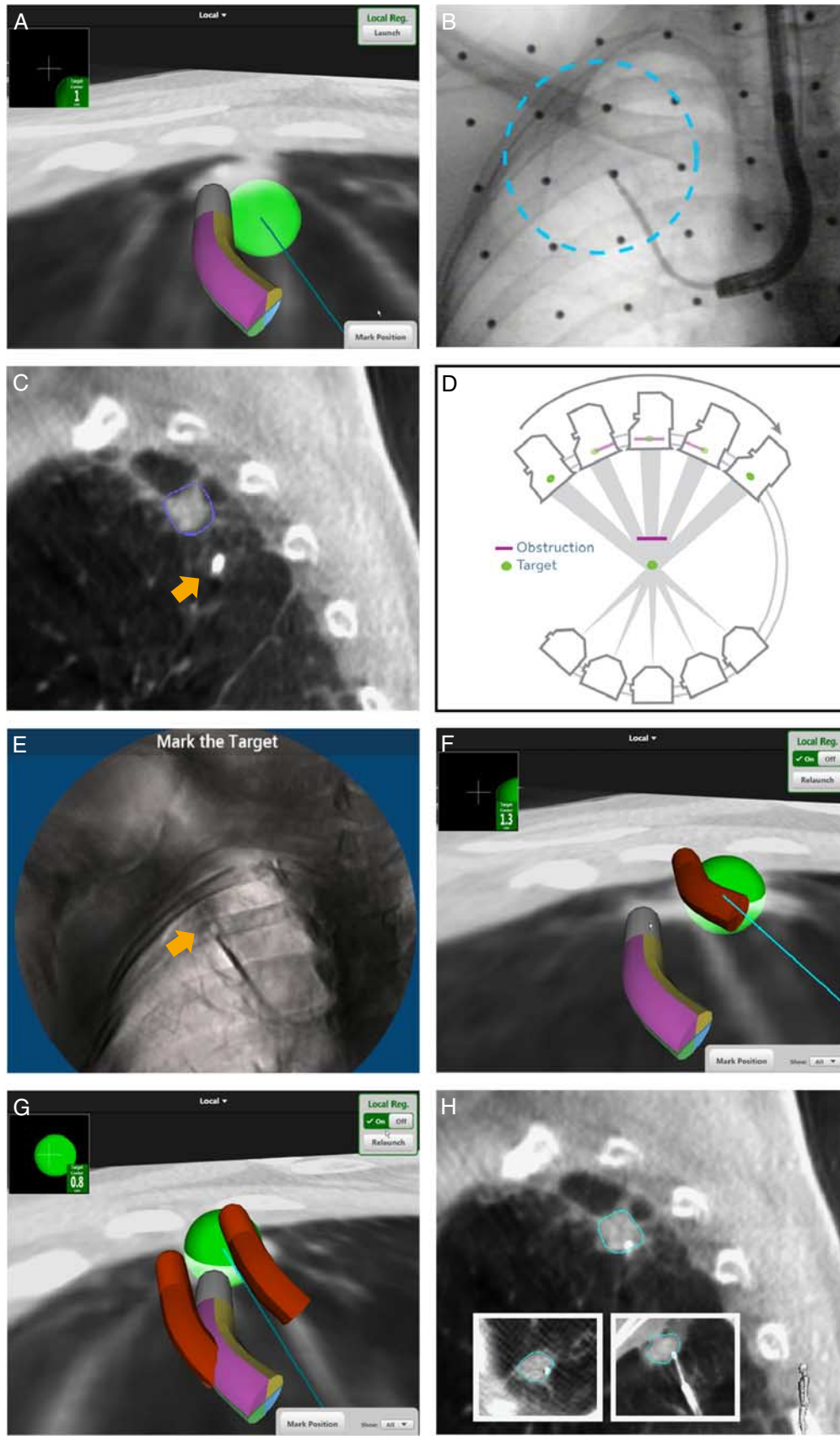

used during the fluoroscopic navigation sweep as shown in Figure 2, with manual adjustment of the adjustable pressure-limiting valve as needed to maintain positive end-expiratory pressure and reduce diaphragmatic movement. Breath-holds were performed at peak inspiration (at the end of a normal tidal breath) and held for 5 to 8 seconds to allow equilibration throughout the bronchial tree before beginning the fluoroscopic navigation sweep.

Study Endpoints and Measures

The primary endpoint was evaluated in technically successful cases (those with local registration complete) as the ability to place the virtual navigation target (green ball) on the actual target lesion. The primary endpoint was calculated as the percentage of cases in which the virtual target was accurately placed to overlap the actual lesion, as confirmed by CBCT, in 3 dimensions. Any case with $>0\%$ overlap was considered a primary endpoint success. Percent overlap between the virtual target and the actual lesion before and after location correction was measured by the study sponsor from the procedure video recordings using a proprietary software algorithm (Fig. 3). The analysis used the procedural recordings to evaluate each 2-dimensional plane (coronal, axial, sagittal) as a grid, comparing the virtual target as marked by the physician during procedure planning with the actual target lesion on CBCT. Three-dimensional volumes were then derived from those 2-dimensional grids, and the overlapping area of the 2 ellipsoids was calculated. This assessment could not be blinded to before versus after location correction. To confirm the accuracy of the target overlap assessment, the distance from the catheter to the center of the target lesion was measured within both fluoroscopic and CBCT images and the magnitude of the difference vector was calculated.

Secondary endpoints were the percentage of 3-dimensional overlap before and after location correction, the ability to correctly identify the intended lesion (as opposed to a nontarget lesion or normal lung tissue), technical success (completion of local registration), procedure time, acquisition of an adequate periprocedural location to begin sampling, adequacy for rapid on-site evaluation (ROSE), and the procedure-day malignancy rate of the ENB-aided sample by ROSE and final pathology. This study was designed as a technical evaluation of location accuracy and did not capture clinical and radiologic follow-up; therefore, true diagnostic yield was not assessed.

All adverse events were captured and evaluated for their relationship to the study procedures and devices. The rates of pneumothorax, bronchopulmonary hemorrhage, and respiratory failure were prespecified secondary endpoints, defined according to the Common Terminology Criteria for Adverse Events (CTCAE) version 5.[25]

Assessments occurred at baseline, and during and immediately after the ENB procedure. Complications were assessed by telephone follow-up 4 to 7 days postprocedure. All primary and secondary endpoints were independently source-data verified.

Statistics

Analyses were performed using SAS Version 9.4 (SAS Inc., Cary, NC) and summarized by descriptive statistics. No formal statistical comparisons or sample size calculations were made for this postmarket feasibility study. The final analysis was conducted after all subjects completed the procedure and the 7-day follow-up.

FIGURE 1. SuperDimension navigation system version 7.2 with fluoroscopic navigation technology. A, Initial navigation on the basis of the preprocedural planning computed tomography and the automatic registration showing the virtual target (green ball) and locatable guide (purple). B, Fluoroscopic image with no visualization of the nodule. C, Sagittal cone-beam computed tomography (CBCT) before correction showing the catheter tip (orange arrow) outside of the target lesion (blue circle). D, Fluoroscopic navigation spin: rotation of the C-arm with continuous fluoroscopy captures 2-dimensional data from various angles around the patient and builds a 3-dimensional volume using a tomosynthesis algorithm. E, Following application of the algorithm and 3-dimensional volume creation, the nodule can now be visualized (orange arrow). F, With the local registration feature turned on, the true spatial relationship between the virtual target (green ball) and the locatable guide (in purple) is seen, before correction of the catheter position. G, After renavigation and correction of the catheter position, showing the locatable guide (in purple) aligned to the target (green ball). The red "ghost" catheters are the marked locations before correction with the local registration feature off (initial navigation) and after correction before realignment. H, Confirmatory sagittal CBCT, with insets for the axial (inset left) and coronal (inset right) views after correction showing the catheter tip inside the target lesion. The 3-dimensional percent overlap between the virtual target and the actual lesion in CBCT was 0% before correction in (C) and 23% after correction in (H). Images courtesy of Dr Michael Pritchett.

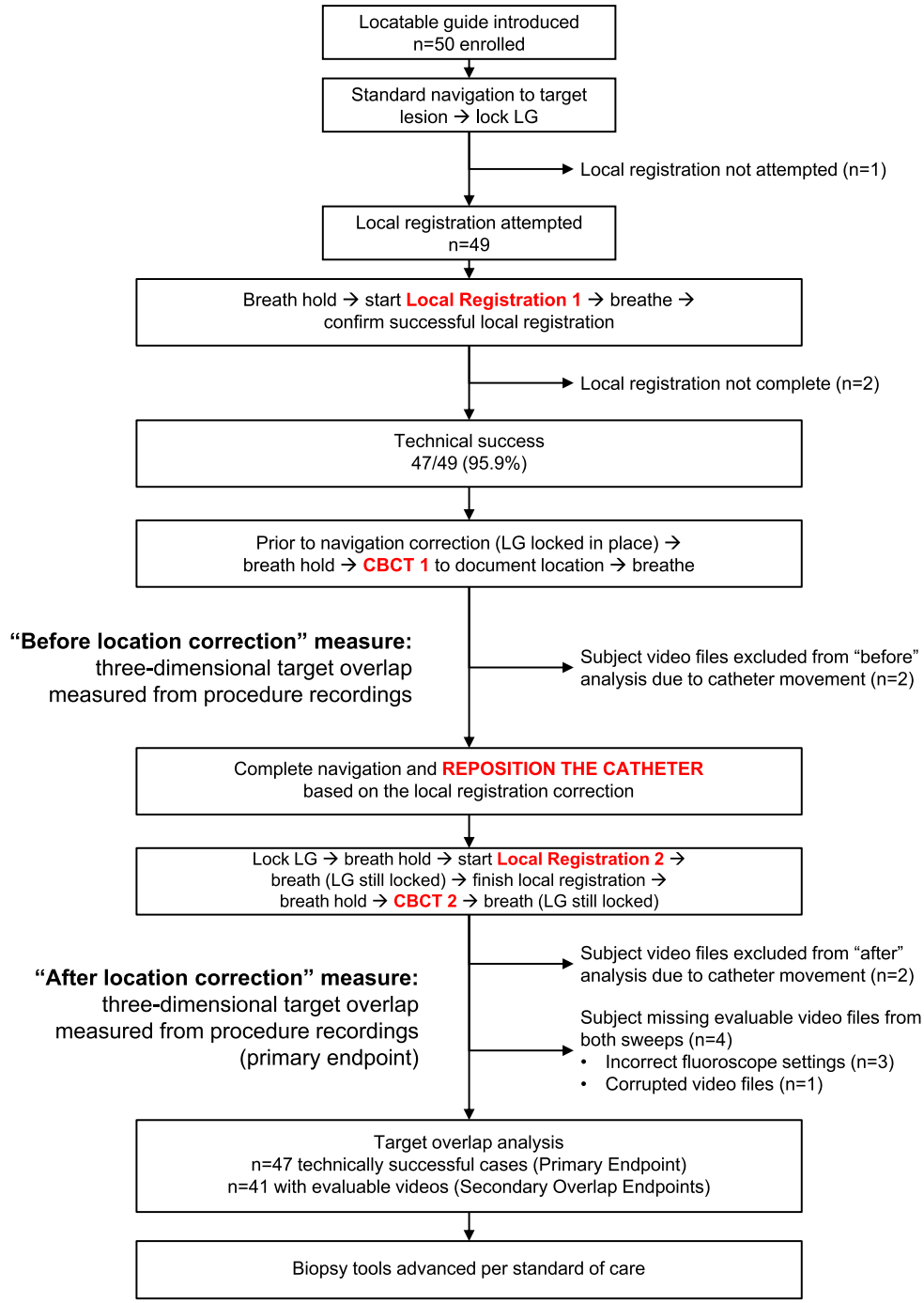

FIGURE 2. Study procedure steps. Following standard navigation to the target lesion (the fluoroscopic navigation system allows local registration within 2.5 cm of the target) the locatable guide (LG) was locked in place and local registration was conducted. Before moving the catheter, cone-beam computed tomography (CBCT) was conducted to allow an analysis of the initial spatial relationship between the virtual target and actual lesion ("before location correction" measure). The catheter was then repositioned on the basis of the local registration, and a second CBCT was conducted to allow an analysis of the updated relationship between the virtual target and actual lesion ("after location correction" measure). Biopsy sampling was then conducted according to standard practice. The primary endpoint was evaluated in all technically successful cases (n = 47). Two subjects from each sweep had to be excluded because of observed movement of the catheter between the fluoroscopy and CBCT sweeps. An additional 4 cases could not be analyzed because of incorrect fluoroscope settings or corrupted files (not because of system error). This resulted in evaluable data sets of 41 subjects per group for the target overlap secondary endpoints.

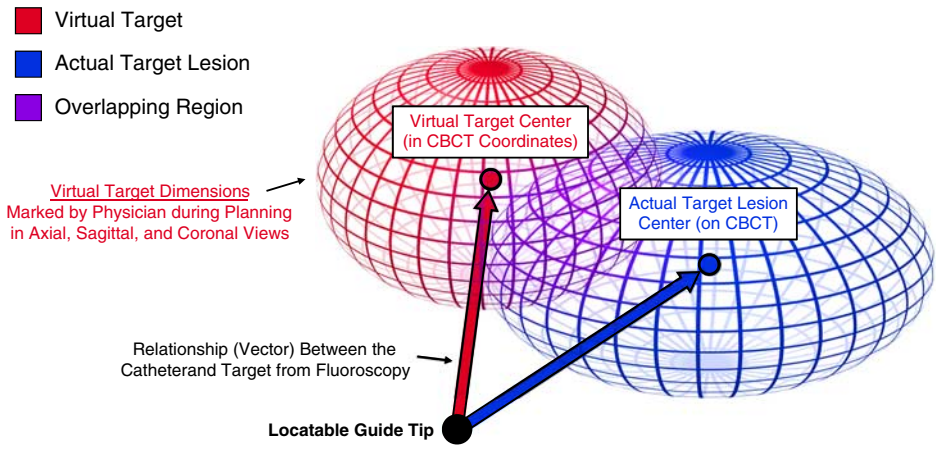

FIGURE 3. Calculation method for 3-dimensional percentage overlap of the virtual target and the actual target lesion. The dimensions of the virtual target (in red) were derived from the dimensions marked by the physician in the coronal, axial, and sagittal views during the planning procedure. The dimensions of the actual target lesion (in blue) in cone-beam computed tomography (CBCT) were derived by manually scrolling through coronal slices to find the lesion center. The boundaries of the 2-dimensional ellipse were marked to calculate the *x*-axis and *y*-axis diameters. Then, the third dimension (*z*-axis) was obtained by scrolling through coronal slices in both directions (positive and negative) to find the beginning and end of the lesion. To calculate the percentage overlap, the locatable guide (LG) tip and target centers were marked on fluoroscopy images to obtain vectors (magnitude and direction relationship) between the LG tip and the target center in fluoroscopy images. Assuming the catheter did not move between the fluoroscopy sweep and the CBCT scan, the target location and size in CBCT coordinates were derived from the calculated vector from fluoroscopy. A software algorithm used the diameters and locations of the targets in CBCT coordinates to calculate the volume of the overlapping area of the 3-dimensional ellipsoids (in purple). Sphere wireframe images adapted from https://commons.wikimedia.org/wiki/File:Sphere_wireframe_10deg_10r.svg under the terms of Creative Commons Attribution 3.0 Unported (CC BY 3.0) (https://creativecommons.org/licenses/by/3.0/deed.en). Adaptations are themselves works protected by copyright. So in order to publish this adaptation, authorization must be obtained both from the owner of the copyright in the original work and from the owner of copyright in the translation or adaptation.

RESULTS

Fifty subjects were enrolled (25 at each of 2 US sites) from August 3, 2018 to February 13, 2019. Demographics, lesion, and procedural characteristics are shown in Table 1. The median lesion size was 17.0 mm. General anesthesia was used in all subjects and inspiratory breath-hold was conducted during all fluoroscopic navigation and CBCT spins in all subjects. Radial endobronchial ultrasound (rEBUS) was used at 1 of the 2 study sites [51.0% (25/49) of subjects] for the standard-of-care biopsy procedure, after all study-specific fluoroscopy and CBCT spins were complete. Cytology brushes were used in 100% (49/49) of cases, aspirating needles in 85.7% (42/49), biopsy forceps in 67.3% (33/49), and bronchoalveolar lavage in 59.2% (29/49). [Specific biopsy tools used were as follows (more than 1 tool was used per subject): Arcpoint pulmonary needle 28.6% (14/49), superDimension aspirating needle 63.3% (31/49), Olympus PeriView FLEX TBNA Needle 49.0% (24/49), superDimension biopsy forceps 63.3% (31/49), Olympus EndoJaw biopsy forceps 4.1% (2/49), GenCut core biopsy system 20.4% (10/49), superDimension cytology brush 95.9% (47/49), other cytology brush 4.1% (2/49), superDimension triple needle cytology brush 4.1% (2/49), and superDimension needle-tipped cytology brush 4.1% (2/49).] The first tool used was the aspirating needle in 53.1% (26/49) and the cytology brush in 46.9% (23/49).

Before initiating the fluoroscopic navigation spin, operators reported that the catheter was in an adequate location to begin biopsy sampling in 93.9% of cases (46/49); meaning, a location in which they would normally have initiated sampling following standard navigation if fluoroscopic navigation were not available. Local registration was attempted in 98.0% (49/50) and completed (technical success) in 95.9% (47/49) (Fig. 2). In the subject without local registration attempted, the fluoroscopic navigation module was opened but the physician decided not to initiate the fluoroscopic navigation sweep because there was no manufacturer-trained radiation technologist available. The subject exited the study without additional data collection. In the 2 subjects in which local registration was incomplete (technical success failures), the fluoroscopic navigation sweep was conducted, but because the

TABLE 1. Subject, Lesion, and Procedural Characteristics (N = 50 Subjects)

Variable	n/N (%) or Mean ± SD (N) [Median] (Min, Max)
Age	69.8 ± 7.7 (50) [70.0] (49.0, 84.0)
Female	35/50 (70.0)
Male	15/50 (30.0)
Race	
White	43/50 (86.0)
Black or African American	5/50 (10.0)
American Indian or Alaska Native	2/50 (4.0)
Chronic obstructive pulmonary disease	31/50 (62.0)
Tobacco use (current or former)	44/50 (88.0)
Lesion size (mm)	20.0 ± 9.6 (49) [17.0] (10.0, 52.0)
Lesions < 20 mm	30/49 (61.2)
Upper lobe location	32/49 (65.3)
Distance from lesion to pleura	10.4 ± 12.2 (49) [5.9] (0.0, 47.4)
Bronchus sign present on CT	26/49 (53.1)
Total procedure time, median (range)* (min)	60 (28-128)
ENB-specific procedure time, median (range)† (min)	54 (18-108)
Fluoroscopic navigation time, median (range)‡ (min)	3.8 (0.2-7.9)

Lesion data are only available in subjects with local registration attempted (49/50).

*Total procedure time: first entry of the bronchoscope to the last exit of the bronchoscope.

†ENB-specific procedure time: first entry of the extended working channel or locatable guide until the last exit of the extended working channel. This includes all study-specific fluoroscopy and CBCT steps which would not normally occur in standard practice.

‡Fluoroscopic navigation time: 2 sweeps pooled. Encompasses C-arm sweep, target marking, and algorithm computational time, inclusive of the initiation of the local registration applet to the time the updated catheter location was ready and on screen (not including CBCT), as measured by the system software.

CT indicates computed tomography; CBCT, cone-beam computed tomography; ENB, electromagnetic navigation bronchoscopy.

correction distance was > 3.0 cm the location of the virtual target was not updated according to the device design. The system therefore performed as designed but because local registration was not completed, these cases were not considered technically successful according to the study definition.

The primary endpoint (3-dimensional target overlap > 0% in all technically successful cases) was achieved in 59.6% (28/47) before location correction and 83.0% (39/47) after location correction. In subjects with evaluable video recordings, target overlap was obtained in 68.3% (28/41) before location correction and 95.1% (39/41) after location correction (Fig. 4). Figure 5 depicts 6 examples of primary endpoint success (Figs. 5A–E) and failure (Fig. 5F). In the 2 cases without target overlap after location correction, diagnoses of malignancy (Fig. 5F) and organizing pneumonia were nonetheless achieved.

The percent of cases without target overlap decreased from 31.7% (13/41) before location correction to 4.9% (2/41) after location correction (Fig. 4). Conversely, the percent of cases with > 50% target overlap increased from 7.3% (3/41) to 24.4% (10/41). The median 3-dimensional percent overlap between the virtual target and the actual lesion in CBCT was 11.4% and 32.8% before and after location correction, respectively. Although the catheter was locked in place, movement between the fluoroscopic navigation sweep and the confirmatory CBCT was possible. However, movement was only observed in 4/100 videos (Fig. 2). As confirmation of the accuracy of the fluoroscopy-based measures relative to CBCT, the median magnitude of the 3-dimensional difference vector between fluoroscopy and the CBCT measures was 6.2 mm (range, 0.0 to 16.6 mm) after location correction. The intended lesion was correctly identified as indicated by the system software 100% (38/38) of cases with sufficient data to assess that endpoint (preprocedural CT files were missing in 3 cases).

ROSE was utilized in 100.0% (49/49) of cases and provided adequate tissue for evaluation in all cases (49/49). On the basis of the ENB-aided sample, malignant results were obtained in 53.1% (26/49) by ROSE and 61.2% (30/49) by final pathology.

CTCAE Grade 1 pneumothorax (no chest tube required) occurred in 1 subject (2%) and scant hemoptysis (CTCAE Grade 1 bronchopulmonary hemorrhage, no interventions required) occurred in 3 subjects (6%). The remaining adverse events were one instance each of viral illness, dizziness, urinary retention, and chronic obstructive pulmonary disease exacerbation, none of which were considered related to the ENB device.

DISCUSSION

ENB is a valuable tool to safely access peripheral lung nodules; however, the diagnostic yield of all guided bronchoscopic techniques that rely on a preprocedural CT scan will be affected by CT-to-body divergence. Although some causes of CT-to-body divergence, such as ventilation technique,[12,22,23] are under the user's control, new technologies are needed to provide intraprocedural location correction.[12]

This study is the first prospective, multicenter analysis of the fluoroscopic navigation technology. Because diagnostic yield is impacted by lesion and procedural factors and varied definitions,[2] the aim of this study was to conduct a technical evaluation of

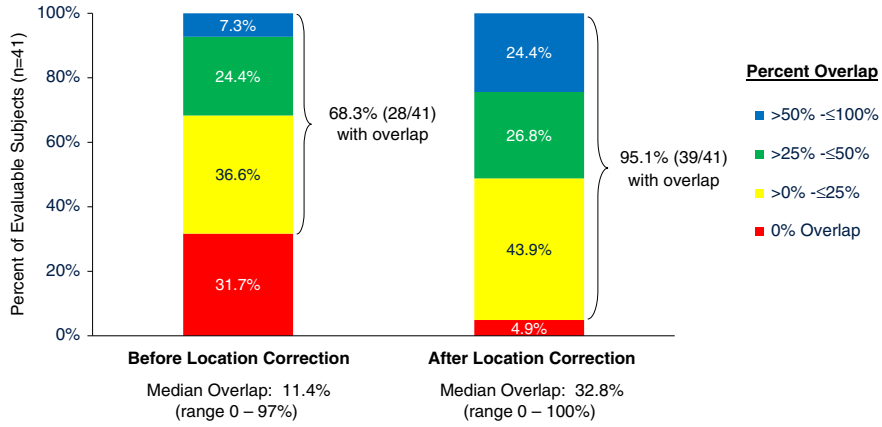

FIGURE 4. Percent overlap in evaluable cases (n = 41) before and after correction of the catheter location on the basis of local registration.

the 3-dimensional location accuracy as confirmed by CBCT. Before local registration, operators considered the catheter to be in an adequate sampling location in 94% of cases. However, when that original virtual target location was compared with the actual 3-dimensional nodule location using

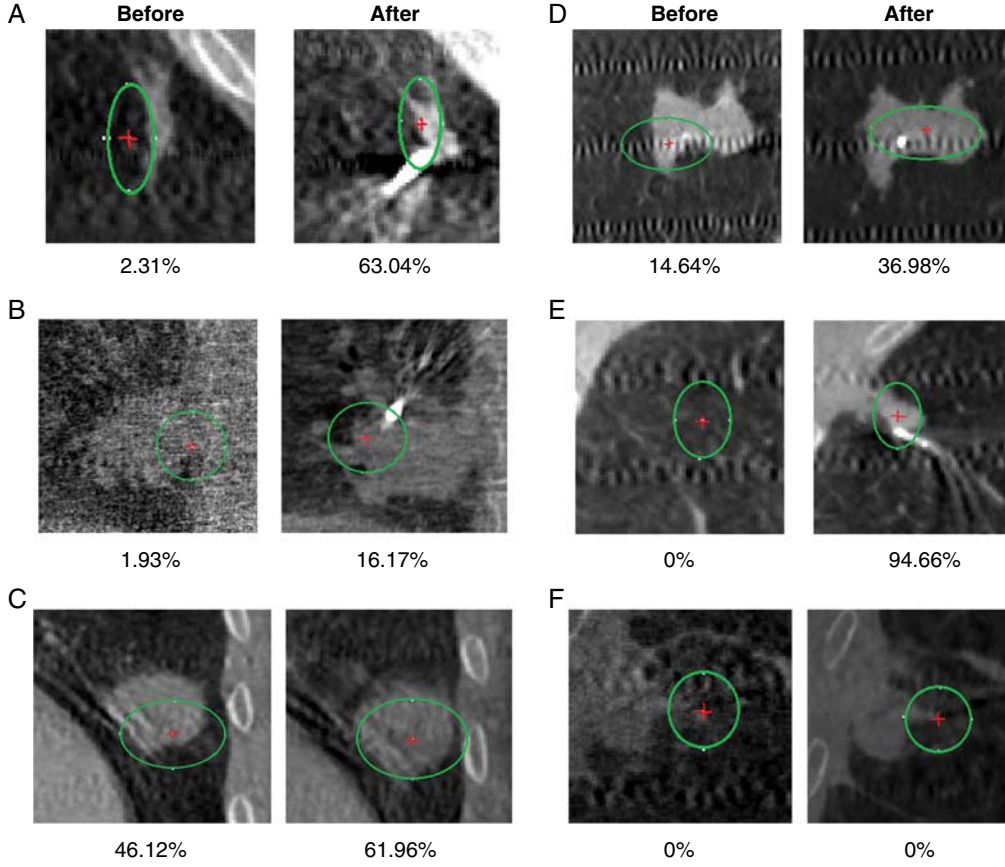

FIGURE 5. Examples of primary endpoint success (A–E) and failure (F) in coronal view. Center of the virtual target (red plus sign) and virtual target (green circle) before and after correction of the catheter location on the basis of local registration. The 3-dimensional percent overlap is shown below each image. Note that while a coronal slice is displayed, the percent overlap was calculated in 3 dimensions. F, The lesion was close to the pleural border and the operator felt pressure against the rib and backed away, yet the catheter was still adequately aligned to obtain a diagnosis.

CBCT, 32% of virtual targets had no overlap with the true target lesion in any dimension. This discrepancy highlights the challenge of CT-to-body divergence in navigation systems that rely solely on a virtual target without intraprocedural imaging confirmation or correction. This finding also underscores the difficulty of evaluating location accuracy by diagnostic yield alone. Following local registration and correction of the catheter position, the virtual target overlapped the actual lesion in 95% of evaluable cases. In the 2 cases without target overlap after location correction, diagnoses of organizing pneumonia and malignancy were still obtained, suggesting that the catheter was positioned to allow clinically relevant target sampling once the biopsy tools were advanced. CBCT confirmation that the biopsy tool is in the lesion is valuable when available. Although prior studies have found that CT-to-body divergence is more pronounced in the lower lobes,[26] we did not find that precorrection target overlap was reduced in lower lobe lesions [69.2% (9/13) lower lobe vs. 67.9% (19/28) upper/middle lobes]. However, this small feasibility study was not powered to allow meaningful conclusions from subset analyses.

Several other technologies currently available or in development seek to mitigate CT-to-body divergence using a variety of methods.[12] None of these systems have evaluated 3-dimensional targeting location accuracy to the same extent as the current study, so direct comparisons are not yet possible. The SPiN Thoracic Navigation System (Veran Medical Technologies, St. Louis, MO) uses respiratory gating and continuous guidance with tip-tracked instruments.[3,27] LungVision (BodyVision Medical Inc., Ramat Ha Sharon, Israel) uses augmented fluoroscopy and dynamic registration tracking.[28] The Lung Suite CBCT system (Philips, Best, The Netherlands) uses live augmented fluoroscopy and position adaptation.[13] Finally, robotic bronchoscopy systems such as the Ion endoluminal robotic system (Intuitive Surgical, Sunnyvale, CA)[8] and the Monarch Platform (Auris Surgical Robotics, Redwood City, CA)[9] use a combination of direct visualization, optical pattern recognition (Monarch platform), and shape sensing (Ion platform) to track the relationship between the catheter and the target lesion in real time. One important consideration in evaluating these new technologies is the method used to provide an accurate "ground truth" of the actual target lesion location in real time during the bronchoscopy procedure. Although common,[29,30] use of rEBUS to confirm lesion localization may not provide an accurate measure of lesion localization. rEBUS accuracy may be confounded by atelectasis and hemorrhage.[10] rEBUS can also only provide a lateral view and not a forward-looking view; thus, rEBUS cannot determine the directionality of the target lesion. Although abstract reports of robotic bronchoscopy have observed rEBUS-confirmed localization success rates of 92% to 96%,[30–32] localization success by rEBUS is not equivalent to diagnostic yield, especially since eccentric rEBUS views in up to 50% of cases[30,32] are associated with significantly lower diagnostic yield.[33,34] A published paper of the Ion robotic platform reported early performance data through 6 months in 29 subjects, with malignant samples in 51.7%, benign samples in 27.6%, and inconclusive results in 20.7% for an early diagnostic yield trend of 79.3%. Eccentric rEBUS image patterns were seen in ~50%; the diagnostic yield in eccentric versus concentric rEBUS patterns was not reported.[8] A multicenter analysis of the Monarch endoscopy platform reported a navigation success rate (rEBUS view or diagnostic tissue obtained) of 89% and a diagnostic yield of 69% (excluding inflammation without follow-up). Diagnostic yields were 81.5%, 72%, and 27% for concentric, eccentric, and absent rEBUS views, respectively. The authors acknowledged that atelectasis resulting in false-positive rEBUS images and lack of long-term follow-up may impact the interpretation of the results, and that true confirmation of navigation success requires CBCT or tool-in-target visualization.[35] CBCT has demonstrated very high diagnostic accuracy when used alone or in combination with other systems; however, access to these systems is currently limited.[13] In an abstract report evaluating the localization accuracy of the LungVision system on the basis of CBCT confirmation, successful navigation was verified by CBCT in 91% of cases despite an initial CT-to-body divergence of 14 mm.[11] Thus, while CBCT is not required to use the fluoroscopic navigation system in standard practice, it provides an accurate and clinically relevant assessment of localization accuracy in 3 dimensions. Of note, a published clinical study of ENB with fluoroscopic navigation found that eccentric and concentric rEBUS views were associated with similar odds of achieving a diagnosis.[17]

The current study was not designed to evaluate diagnostic yield because it did not include clinical and radiologic follow-up of initially nonmalignant results. However, the ENB-aided

malignancy rate of 61.2% is similar to or higher than previous ENB studies. In the NAVIGATE study (which used prior versions 6.3 to 7.1 of this ENB system), the malignancy rate was 44% on the basis of the initial ENB-aided sample and 67% at 1 year (including false negatives).[2] Aboudara et al[17] reported an ENB-aided malignancy rate of 53.7% using the fluoroscopic navigation system. These outcomes are dependent upon the prevalence of malignancy in the patient population and would need to be proven with longer-term follow-up in future studies.

LIMITATIONS

This feasibility study was conducted at only 2 centers and enrolled a relatively small number of patients. The results will need to be confirmed in a larger, unrestricted cohort. Missing video files in 8 patients reduced the size of the evaluable data set and could have biased the results; however, the primary endpoint used the most conservative estimate and assumed that all missing cases did not have target overlap. The percentage overlap calculation also was not blinded to procedural technique. Care was taken to ensure identical ventilation strategies throughout each case, including during each breath-hold; however, minimal changes are reasonably possible because of uncontrolled factors. Finally, this study was designed as a technical feasibility analysis of target lesion overlap and was not designed to assess diagnostic yield. Larger, multicenter, randomized studies are necessary to confirm these results and understand the impact of this technology on diagnostic yield.

CONCLUSIONS

This study suggests that ENB using enhanced tomosynthesis-based visualization and local correction safely improves the 3-dimensional convergence between the virtual target and the actual lung lesion as imaged in CBCT. Mitigation of CT-to-body divergence may improve localization and increase diagnostic yield compared with platforms that do not utilize intraprocedural imaging with local registration.

ACKNOWLEDGMENTS

The authors acknowledge Sean Pidgeon, Dana Glozman, and Yun Bai, of Medtronic (Minneapolis, MN) for providing data and biostatistical analysis. Medical writing support was provided by Kristin Hood PhD of Medtronic in accordance with Good Publication Practice guidelines and under the full direction of the authors.

REFERENCES

1. Mehta AC, Hood KL, Schwarz Y, et al. The evolutional history of electromagnetic navigation bronchoscopy. *Chest*. 2018;154:935–947.
2. Folch EE, Pritchett MA, Nead MA, et al. Electromagnetic navigation bronchoscopy for peripheral pulmonary lesions: one-year results of the prospective, multicenter navigate study. *J Thorac Oncol*. 2019;14:445–458.
3. Belanger AR, Burks AC, Chambers DM, et al. Peripheral lung nodule diagnosis and fiducial marker placement using a novel tip-tracked electromagnetic navigation bronchoscopy system. *J Bronchology Interv Pulmonol*. 2019;26:41–48.
4. Hogarth D, Bhadra K, Whitten P, et al. A novel endobronchial fluoroscopic navigation and localization system: a summary of a multicenter LungVision trial. *Chest*. 2018;154:880A–882A.
5. Eberhardt R, Kahn N, Gompelmann D, et al. LungPoint—a new approach to peripheral lesions. *J Thorac Oncol*. 2010;5:1559–1563.
6. Herth FJ, Eberhardt R, Sterman D, et al. Bronchoscopic transparenchymal nodule access (BTPNA): first in human trial of a novel procedure for sampling solitary pulmonary nodules. *Thorax*. 2015;70:326–332.
7. Ali EAA, Takizawa H, Kawakita N, et al. Transbronchial biopsy using an ultrathin bronchoscope guided by cone-beam computed tomography and virtual bronchoscopic navigation in the diagnosis of pulmonary nodules. *Respiration*. 2019;98:321–328.
8. Fielding DIK, Bashirzadeh F, Son JH, et al. First human use of a new robotic-assisted fiber optic sensing navigation system for small peripheral pulmonary nodules. *Respiration*. 2019;98:142–150.
9. Rojas-Solano JR, Ugalde-Gamboa L, Machuzak M. Robotic bronchoscopy for diagnosis of suspected lung cancer: a feasibility study. *J Bronchology Interv Pulmonol*. 2018;25:168–175.
10. Casal RF, Sarkiss M, Jones AK, et al. Cone beam computed tomography-guided thin/ultrathin bronchoscopy for diagnosis of peripheral lung nodules: a prospective pilot study. *J Thorac Dis*. 2018;10:6950–6959.
11. Pritchett M. Comparison of pulmonary nodule location between preprocedural CT and intra-procedural cone-beam CT during guided bronchoscopy. *J Thorac Oncol*. 2018;13:S403.
12. Pritchett MA, Bhadra K, Calcutt M, et al. Virtual or reality: divergence between preprocedural computed tomography scans and lung anatomy during guided bronchoscopy. *J Thorac Dis*. 2020;12:1595–1611.
13. Pritchett MA, Schampaert S, de Groot JAH, et al. Cone-beam CT with augmented fluoroscopy combined with electromagnetic navigation bronchoscopy for biopsy of pulmonary nodules. *J Bronchology Interv Pulmonol*. 2018;25:274–282.
14. Thiboutot J, Lee HJ, Silvestri GA, et al. Study design and rationale: a multicenter, prospective trial of electromagnetic bronchoscopic and electromagnetic transthoracic navigational approaches for the biopsy of peripheral pulmonary nodules (ALL IN ONE Trial). *Contemp Clin Trials*. 2018;71:88–95.
15. ClinicalTrials.gov. Clinical utility for ion endoluminal system (NCT03893539). Available at: https://clinicaltrials.gov/ct2/show/NCT03893539. Accessed June 17, 2019.

16. ClinicalTrials.gov. Evaluation of the Archimedes™ system for transparenchymal nodule access 2 (EAST2) (NCT02867371). Available at: https://clinicaltrials.gov/ct2/show/NCT02867371. Accessed August 30, 2019.
17. Aboudara M, Roller L, Rickman O, et al. Improved diagnostic yield for lung nodules with digital tomosynthesis-corrected navigational bronchoscopy: initial experience with a novel adjunct. *Respirology*. 2020;25:206–213.
18. Barak R, Weingarten OP, Greenburg B, et al. System and method for navigating to target and performing procedure on target utilizing fluoroscopic-based local three dimensional volume reconstruction. Inventors; US patent 2017/0035380 A1, assignee. February 9, 2017.
19. Weingarten OP, Barak R, System and method for local three dimensional volume reconstruction using a standard fluoroscope. Inventors; US patent 2017/0035379 A1, assignee. February 9, 2017.
20. Ferrari A, Bertolaccini L, Solli P, et al. Digital chest tomosynthesis: the 2017 updated review of an emerging application. *Ann Transl Med*. 2018;6:91.
21. Nelson G, Wu M, Hinkel C, et al. Improved targeting accuracy of lung tumor biopsies with scanning-beam digital x-ray tomosynthesis image guidance. *Med Phys*. 2016;43:6282–6290.
22. Rusca M, Proietti S, Schnyder P, et al. Prevention of atelectasis formation during induction of general anesthesia. *Anesth Analg*. 2003;97:1835–1839.
23. Coussa M, Proietti S, Schnyder P, et al. Prevention of atelectasis formation during the induction of general anesthesia in morbidly obese patients. *Anesth Analg*. 2004:1491–1495.
24. Brismar B, Hedenstierna G, Lundquist H, et al. Pulmonary densities during anesthesia with muscular relaxation–a proposal of atelectasis. *Anesthesiology*. 1985;62:422–428.
25. National Cancer Institute, Cancer Therapy Evaluation Program, United States Department of Health and Human Services, National Institutes of Health. Common Terminology Criteria for Adverse Events (CTCAE) Version 5.0. Available at: https://ctep.cancer.gov/protocolDevelopment/electronic_applications/ctc.htm#ctc_50. Accessed January 23, 2018.
26. Chen A, Pastis N, Furukawa B, et al. The effect of respiratory motion on pulmonary nodule location during electromagnetic navigation bronchoscopy. *Chest*. 2015;147:1275–1281.
27. Mallow C, Lee H, Oberg C, et al. Safety and diagnostic performance of pulmonologists performing electromagnetic guided percutaneous lung biopsy (SPiNperc). *Respirology*. 2019;24:452–458.
28. Hogarth DK. Use of augmented fluoroscopic imaging during diagnostic bronchoscopy. *Future Oncol*. 2018;14:2247–2252.
29. Cicenia J, Sethi S. Navigation to peripheral lung nodules using an artificial intelligence-driven augmented image fusion platform (LungVision): a pilot study. *Chest*. 2019;156:A830.
30. Chen A, Pastis N, Mahajan A, et al. Multicenter, prospective pilot and feasibility study of robotic-assisted bronchoscopy for peripheral pulmonary lesions. *Chest*. 2019;156:A2260–A2261.
31. Chen AC, Pastis NJ, Mahajan AK, et al. Multicenter, prospective pilot and feasibility study of robotic assisted bronchoscopy for peripheral pulmonary lesions. *Am J Respir Crit Care Med*. 2019;199:A7304.
32. Chaddha U, Kovacs SP, Manley C, et al. Robot-assisted bronchoscopy for lung nodule diagnosis: a pilot feasibility study. *Am J Respir Crit Care Med*. 2019;199:A1266.
33. Tanner NT, Yarmus L, Chen A, et al. Standard bronchoscopy with fluoroscopy vs thin bronchoscopy and radial endobronchial ultrasound for biopsy of pulmonary lesions: a multicenter, prospective, randomized trial. *Chest*. 2018;154:1035–1043.
34. Chen A, Chenna P, Loiselle A, et al. Radial probe endobronchial ultrasound for peripheral pulmonary lesions. A 5-year institutional experience. *Ann Am Thorac Soc*. 2014;11:578–582.
35. Chaddha U, Kovacs SP, Manley C, et al. Robot-assisted bronchoscopy for pulmonary lesion diagnosis: results from the initial multicenter experience. *BMC Pulm Med*. 2019;19:243.

